

CONF-790968--4

MEASUREMENTS OF  $Q_{\beta}$  FOR NEUTRON-DEFICIENT NUCLEI WITH  $A \sim 80^*$ 

P. E. Haustein, C. J. Lister, D. E. Alburger,  
and J. W. Olness

Brookhaven National Laboratory  
Upton, NY 11973 USA

## INTRODUCTION

Measurement of the decay energies ( $Q_{\beta}$ ) of isotopes which are far removed from the valley of beta stability permits checks of mass theories and provides input for the refinement of mass systematics. In particular, the nuclei which lie on or near the  $N = Z$  line with  $A > 60$  are expected to provide some of the most stringent tests of these theories. The nuclei in this region are expected to highlight the influences of a variety of nuclear structure features which affect the nature of the mass surface. These include isospin effects, the influences of nuclear shells on binding energies, single particle versus collective phenomena, coulomb energy considerations, symmetry effects, and the role of nuclear deformation in regions of unusual  $N/Z$  ratio. In addition to the delineation of the mass surface in these regions, spectroscopic studies of nuclei which lie off of the beta stability line permit additional tests of the detailed predictions of nuclear structure theories.

Neutron deficient nuclei around  $^{80}\text{Zr}$  constitute a rather poorly characterized region with only fragmentary decay properties reported for the isotopes in this region and minimal mass-excess or decay energy data available at the present time. Of particular interest in this region is the rapid change which occurs in the excitation energy of the first  $2^+$  levels in even-even nuclei. The sharp depression<sup>1</sup> in this quantity for  $Z \sim 40$  and  $N \sim 40$  is taken as evidence for exceptionally large oblate deformation for these nuclides.

\*Research performed at Brookhaven National Laboratory under contract with the U.S. Department of Energy.

MASTER

## DISCLAIMER

**This report was prepared as an account of work sponsored by an agency of the United States Government. Neither the United States Government nor any agency Thereof, nor any of their employees, makes any warranty, express or implied, or assumes any legal liability or responsibility for the accuracy, completeness, or usefulness of any information, apparatus, product, or process disclosed, or represents that its use would not infringe privately owned rights. Reference herein to any specific commercial product, process, or service by trade name, trademark, manufacturer, or otherwise does not necessarily constitute or imply its endorsement, recommendation, or favoring by the United States Government or any agency thereof. The views and opinions of authors expressed herein do not necessarily state or reflect those of the United States Government or any agency thereof.**

## **DISCLAIMER**

**Portions of this document may be illegible in electronic image products. Images are produced from the best available original document.**

Earlier studies<sup>2</sup> of the nuclei in this region were performed off line with radioactive sources which had been produced by a variety of heavy-ion reactions on targets of normal isotopic distribution. These production reactions were, in general, performed at energies well above that of the coulomb barrier. Isotopic assignments were made in many cases with the assumption that the dominant reaction channel was (HI,Xn). However at the reported bombarding energies this assumption is dubious because evaporation calculations and reaction systematics indicate that proton and alpha particle emission competes fully with neutron evaporation. Conflicting reports<sup>3,4</sup> on the decay properties of <sup>79</sup>Sr and the reported<sup>5</sup> observation of anomalously long half-lives for nuclides, e.g. <sup>78</sup>Sr, with high predicted decay energies led to a decision to reinvestigate this mass region.

The present study has resulted in the observation of a new isotope, <sup>80</sup>Y,  $T_{1/2} = 34$  secs, as well as a general investigation of the decay properties of several nuclei in this region. Measurements of the total decay energy of <sup>80</sup>Y and neighboring nuclides serve to explore the interplay between the mass surface and the extent of nuclear deformation as well as providing the first definitive checks of mass theory predictions in this region. During the course of these investigations a preliminary report on a similar study was published<sup>6</sup> by the French group of Della Negra et al.

## EXPERIMENTAL

### Techniques

One of the most convenient methods for the production of neutron-deficient nuclei with  $N \sim Z$ ,  $A \sim 80$  is by means of heavy-ion reactions of the type <sup>24</sup>Mg + <sup>58</sup>Mg, <sup>24</sup>Mg + <sup>60</sup>Ni, or <sup>40</sup>Ca + <sup>40</sup>Ca. The excitation energy of the compound nucleus is kept low and carefully adjusted to maximize the yield of the one or two reaction products of interest which result from the evaporation of just a few nucleons from the relatively "cold" compound system. Intercomparison of "in-beam"  $\gamma$ -ray yields from these reactions with predictions from evaporation calculations are then used to establish relative excitation functions for various reaction channels and to select optimum bombarding energies. These results, in combination with the  $\gamma$ -ray spectra and half-life measurements which are obtained from the radioactive sources prepared from the same reactions, serve to establish isotopic assignments for the products of interest. Energy level schemes are then developed from the analysis of ( $\gamma, \gamma, t$ ) coincidence spectra. Total decay energy measurements ( $Q_\beta$ ) are obtained by ( $\beta^+, \gamma$ ) coincidence spectroscopy. Plastic  $\gamma$ -ray detectors are calibrated with several radioactive sources (e.g. <sup>27</sup>Si or <sup>58</sup>Cu) whose endpoints spanned the expected endpoint energies of the

nuclides of interest. The shapes of these "standard" beta-ray spectra are then used as input to a stretching algorithm which permits the determination of endpoint energies of other  $\beta$ -ray spectra by comparison to expanded or contracted versions of the "standard" spectra. In general,  $Q_\beta$  values for each isotope of interest are determined from weighted averages of endpoint energies obtained from several selected  $\gamma$ -ray gates.

### Apparatus

The helium jet recoil transfer technique was employed as a means of continuously preparing essentially massless radioactive sources for  $\beta$ - and  $\gamma$ -ray spectroscopy. Heavy-ion beams from the BNL tandem Van de Graaff facility were collimated and focussed onto targets of natural Ni with thicknesses of 0.6-2.5 mg/cm<sup>2</sup>. Recoil products which emerged from the target were thermalized in helium to which small admixtures of water vapor and isopentyl alcohol had been added by a bubbler system to improve transport efficiency. Using a modified version of a target and recoil collection chamber which has been described<sup>7</sup> previously, the products were collected after thermalization into a multiple capillary bundle which consisted of six stainless steel needles. The helium flow from the capillary bundle was combined into a single capillary of the same size and the resulting flow was directed through a shielding wall from the irradiation station to the counting area by means of polyethylene surgical tubing. At the counting station<sup>8</sup> the helium was skimmed off and pumped away. The recoil products were then deposited onto an aluminized Mylar tape loop. The tape could be advanced from the position where the recoil products were deposited onto it to a counting area 30.5 cm away in 0.2 sec by means of a sprocket-fed photoelectric reader system. At the counting location detectors could be placed to within  $\sim$ 6 mm of the tape:  $\beta$  and  $\gamma$  rays emerged from the sources on the tape through a 17 mg/cm<sup>2</sup> Mylar window. The time periods during which the tape was stopped for counting of one source and collection of the next could be varied. In this way the collection/counting system could be "tuned" to enhance the observation of isotopes with particular half lives. The periodic removal of the sources from the detector area in this sample shuttling procedure effectively eliminated interference from long-lived daughter activities. Except for the rare gas isotopes of Kr, the helium-jet system produced high intensity sources with little or no variation in yield from element to element. Figure 1 shows a schematic view of the helium-jet system.

Data acquisition was accomplished with commercial Ge(Li) and plastic detectors and standard analog electronics. Coincidence  $\gamma$ -ray spectra were accumulated through "fast-slow" logic networks and along with a TAC output for gating of prompt and delayed cascades,

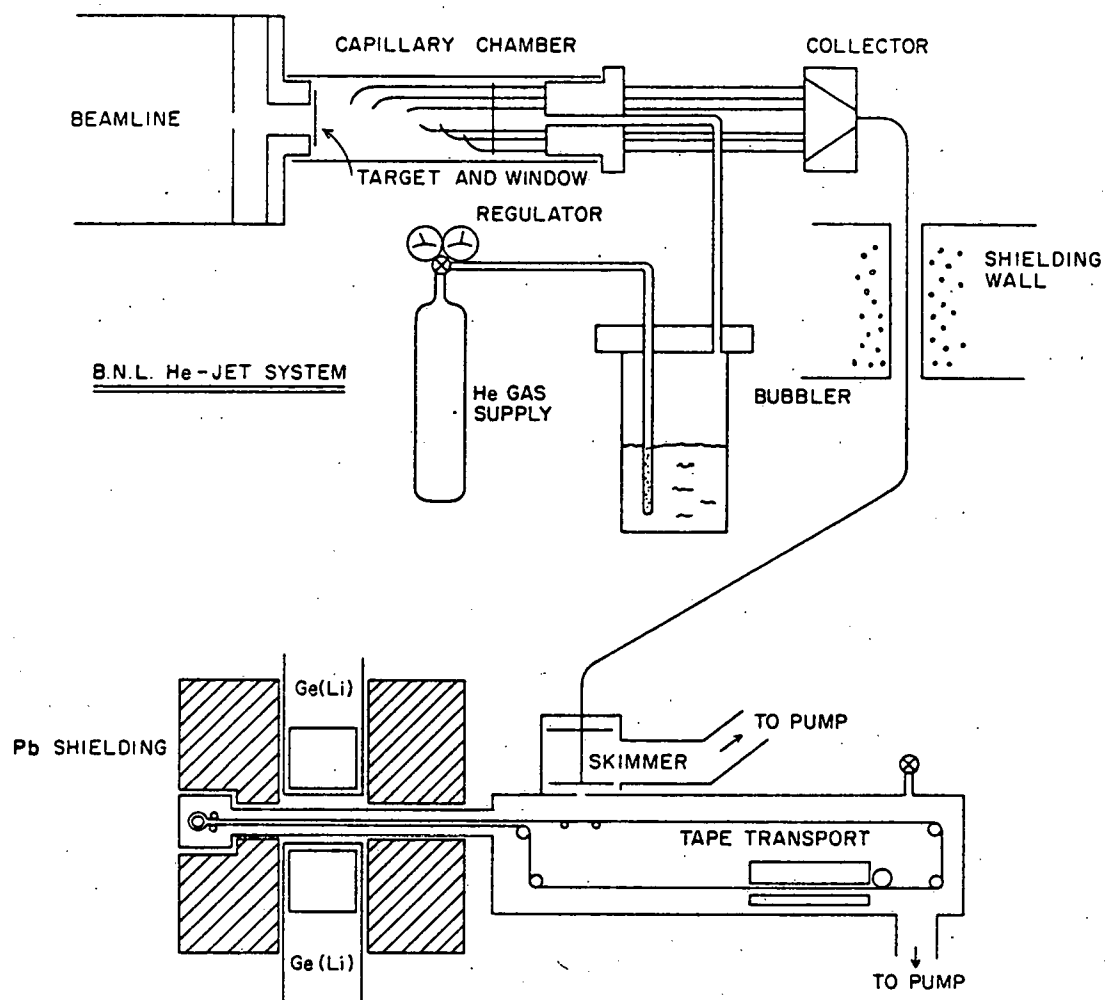


Fig. 1. Schematic view of the helium-jet system.

the coincidence events were written serially onto magnetic tape on a Sigma-7 computer for later off-line sorting. Singles spectra could be recorded in a similar way with a time-from-shuttle parameter included to permit the generation of decay curve data.

## RESULTS

Gamma-ray spectra of radioactive sources which had been produced by the  $^{24}\text{Mg} + ^{58}\text{Ni}$  reaction ( $E_{\text{lab}} = 75 \text{ MeV}$ ) revealed the presence of several products, e.g.,  $^{76-79}\text{Rb}$  and  $^{80}\text{Sr}$ . In addition, several other lines were observed. These could be attributed to either the

decay of  $^{79}\text{Sr}$  or to the decay of a new isotope  $^{80}\text{Y}$ , since the  $\gamma$ -lines in the radioactive sources were of the same energy as transitions which have been reported<sup>2</sup> to result from de-excitation of the ground state rotational band in  $^{80}\text{Sr}$ . Examination of  $\gamma$ -ray spectra from both radioactive sources and "in-beam" studies was made as a function of incident bombarding energy in order to construct relative excitation functions for these activities and to compare these to a statistical evaporation code. In general,  $\gamma$ -rays were attributed to the decays of either  $^{79}\text{Sr}$  or  $^{80}\text{Y}$  on the basis of half-life, excitation, and/or coincidence data. These results are summarized in Table 1. A decay scheme for  $^{80}\text{Y}$  is shown in Fig. 2. It was developed from coincidence spectra; energy level ordering and the beta-ray feeding pattern were deduced from the  $\gamma$ -ray population and depopulation through levels in the daughter nucleus.

Positron spectra from  $^{79}\text{Sr}$ ,  $^{80}\text{Y}$ , and  $^{82}\text{Y}$ , several neutron deficient Rb activities, and calibration sources such as  $^{27}\text{Si}$  and  $^{58}\text{Cu}$  (which had also been produced and transported in the He-jet system) were accumulated using a plastic scintillator. Two such calibration spectra are shown in Fig. 3; the insert shows the stretch factor  $\alpha$ , ( $E = A + B\alpha$ ) as a function of energy. It was used to compress or expand the calibration spectra and these were

Table 1. Half-lives, Gamma-ray Energies, and Relative Intensities in the Decays of  $^{79}\text{Sr}$  and  $^{80}\text{Y}$

Isotope	$T_{1/2}$	$E_{\gamma}$ (keV)	$I_{\gamma}$ (relative)
$^{79}\text{Sr}$	$2.30 \pm 0.10$ min	$104.97 \pm 0.12$	100
		$140.98 \pm 0.14$	29
		$219.62 \pm 0.15$	20
		$507.55 \pm 0.15$	16
$^{80}\text{Y}$	$33.8 \pm 0.6$ sec	$385.87 \pm 0.10$	100
		$595.06 \pm 0.15$	43
		$690.50 \pm 0.35$	3
		$756.48 \pm 0.13$	11
		$782.81 \pm 0.16$	6
		$851.90 \pm 0.15$	9
		$1105.80 \pm 0.30$	4
		$1185.22 \pm 0.15$	15
		$1267.67 \pm 0.35$	5
		$1277.52 \pm 0.35$	3
$1394.55 \pm 0.45$	1		

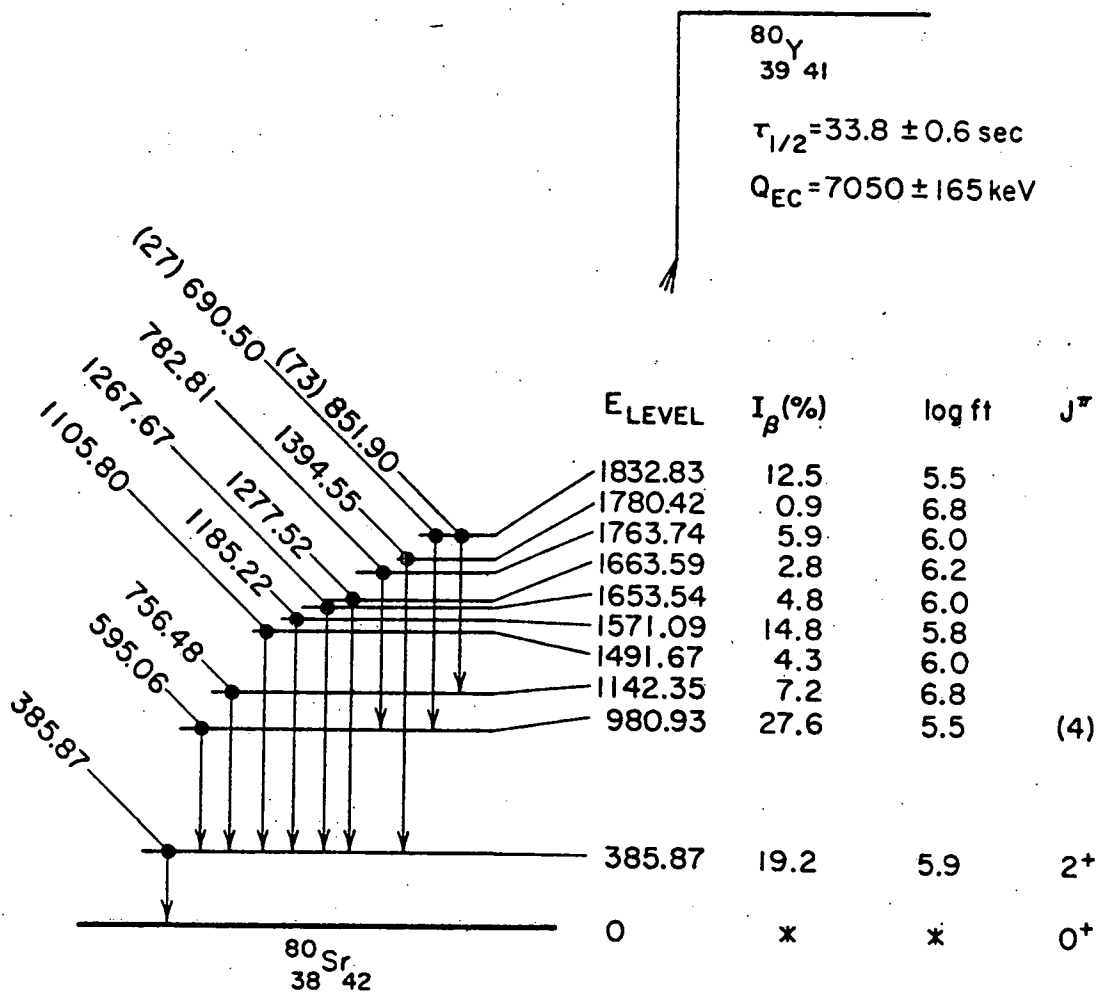


Fig. 2. Decay scheme for  $^{80}\text{Y}$ .

then used as standard shapes and fitted to positron spectra of  $^{79}\text{Sr}$ ,  $^{80}\text{Y}$ , or  $^{82}\text{Y}$ , e.g. Fig. 4.  $Q_{EC}$  values were thus determined by this method. In estimating errors, contributions from the fitting procedure, the statistical quality of both the calibration and "unknown" spectra and the linearity and reproducibility of the detector response were included. Table 2 lists the experimentally determined  $Q_{EC}$  for  $^{79}\text{Sr}$ ,  $^{80}\text{Y}$ , and  $^{82}\text{Y}$  along with predictions from several atomic mass theories.<sup>9,10</sup>

#### DISCUSSION

The experimentally determined value of  $5.07 \pm 0.07 \text{ MeV}$  for the  $Q_{EC}$  of  $^{79}\text{Sr}$  compares most closely with the prediction<sup>9</sup> of 5.14 MeV

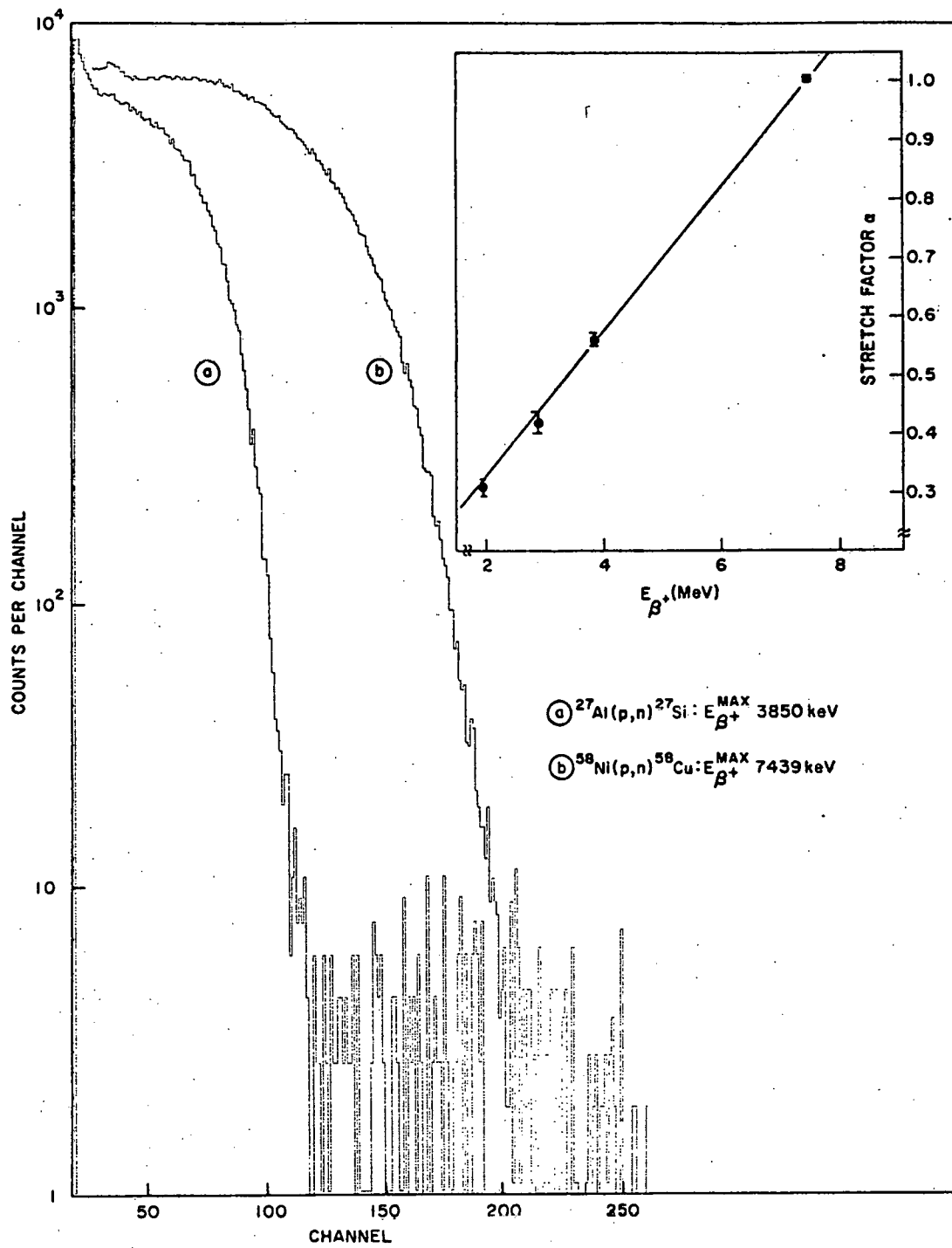


Fig. 3. Positron calibration spectra of  $^{27}\text{Si}$  and  $^{58}\text{Cu}$ . The insert shows the energy dependence of the stretch factor  $\alpha$ .

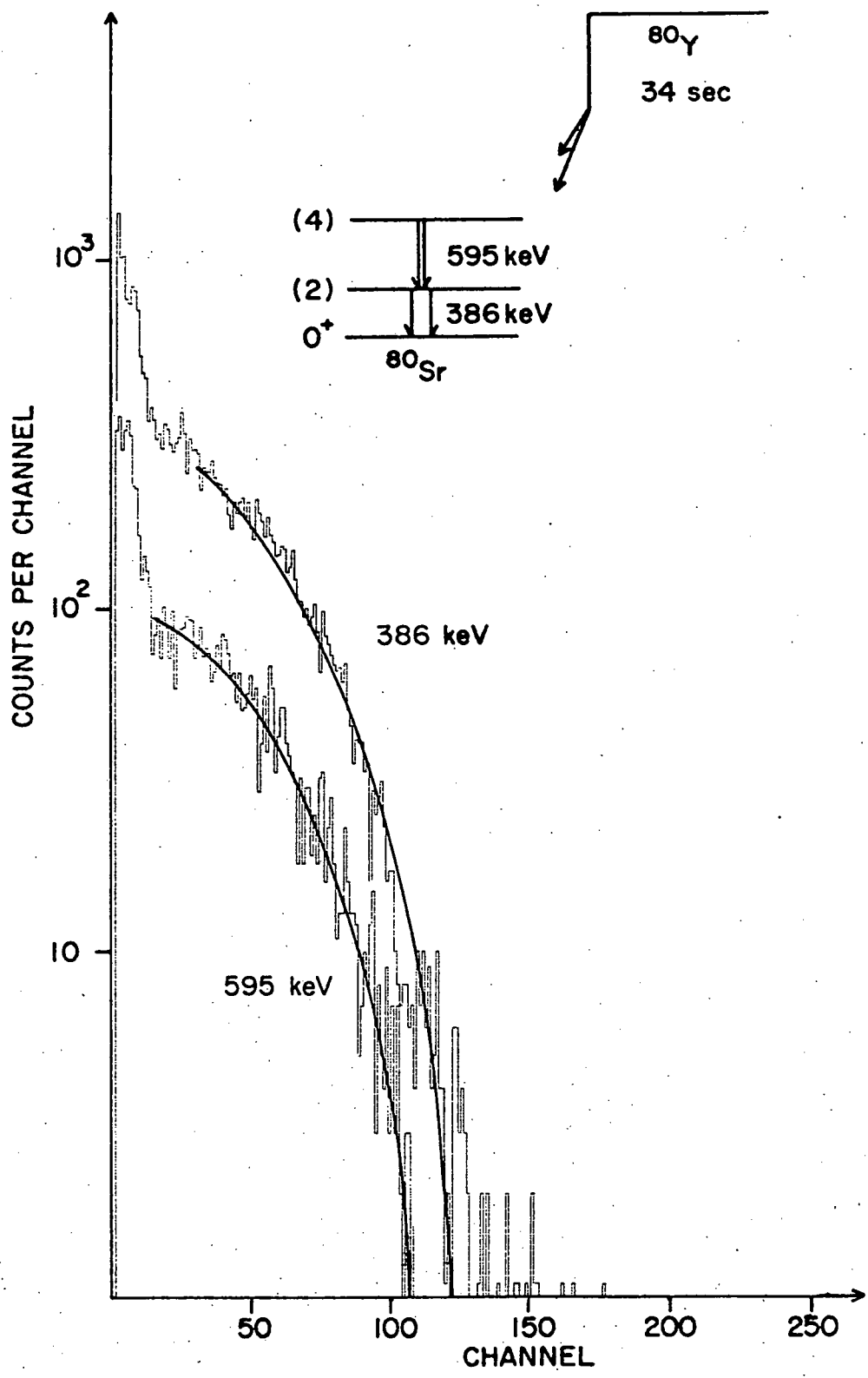


Fig. 4. Positron spectra from the decay of <sup>80</sup>Y.

Table 2. Experimental and Predicted QEC in MeV

Isotope	$^{79}_{38}\text{Sr}$	$^{80}_{39}\text{Y}$	$^{82}_{39}\text{Y}$
Experiment	$5.07 \pm 0.07$	$7.05 \pm 0.17$	$7.75 \pm 0.09$
Myers <sup>a</sup>	5.14	8.74	7.18
Groote, Hilf, Takahaski <sup>a</sup>	5.41	8.80	7.22
Seeger, Howard <sup>a</sup>	5.5	9.1	7.6
Liran, Zeldes <sup>a</sup>	6.05	10.42	8.58
Beiner, Lombard, Mas <sup>a</sup>	6.0	---	---
Jänecke, Garvey, Kelson <sup>a</sup>	5.88	9.85	8.25
Comay, Kelson <sup>a</sup>	5.39	9.74	8.28
Jänecke, Eynon <sup>a</sup>	5.72	9.62	7.99
Monahan, Serduke <sup>b</sup>	6.09	10.10	8.25
Predicted average	5.68	9.55	7.92

<sup>a</sup>Ref. 9.

<sup>b</sup>Ref. 10.

of the Myers Semiempirical Droplet Model. It is however lower than all of the predictions by up to  $\sim 1$  MeV. Since this is of the order of the spread in the predictions, the experimentally measured QEC of  $^{79}\text{Sr}$ , by itself, sheds little light on the predictive properties of the presently available mass models. The cases of  $^{80}\text{Y}$  is, however, more instructive. Predictions for the  $^{80}\text{Y}$  decay energy range from 8.74 to 10.42 MeV with an average of 9.55 MeV. Over 2.5 MeV separates the experimental result of  $7.05 \pm 0.17$  MeV from this average with all of the predictions indicating significantly higher decay energy than that observed. Examination of QEC values determined from our data for several well characterized Rb and Sr activities which were produced along with  $^{79}\text{Sr}$  and  $^{80}\text{Y}$  in our experiment show general agreement with earlier work. The measured QEC for  $^{82}\text{Y}$  ( $T_{1/2} = 9.5$  sec) of  $7.85 \pm 0.09$  MeV, for example, is correctly predicted (QEC<sup>ave</sup> = 7.92 MeV). This tends to discount the possibility of any large systematic errors in our measurements.

It is clearly of interest to extend measurements of this type to other nuclei in this region, especially those further removed from the stability line. The region near  $^{80}\text{Zr}$  appears to be one of rapidly changing nuclear deformation and enhanced collective effects

The low QEC of  $^{80}\text{Y}$  may be a signature of such phenomena as they relate to sensitivity of the mass surface to nuclear deformation.

#### REFERENCES

1. E. Nolte, Y. Shida, W. Kutschera, R. Prestele, and H. Morinaga, *Z. Physik*, 268:267 (1974).
2. C. M. Lederer and V. S. Shirley, "Table of Isotopes," Wiley & Sons, New York (1978) 7th ed.
3. A. N. Bilge and G. G. J. Boswell, *J. Inorg. Nucl. Chem.*, 33:2251 (1974).
4. I. M. Ladenbauer-Bellis, H. Bakhru, and B. Jones, *Can. J. Phys.*, 50:3071 (1972).
5. A. N. Bilge and G. G. J. Boswell, *J. Inorg. Nucl. Chem.*, 33:4001 (1971).
6. Annual Report (1978), Institut de Physique Nucléaire, Division de Radiochimie, Université Paris-Sud.
7. R. E. Leber, P. E. Haustein, and I.-M. Ladenbauer-Bellis, *J. Inorg. Nucl. Chem.*, 38:951 (1976).
8. D. E. Alburger and T. G. Robinson, *Nucl. Instr. Methods.*, 164:507 (1979).
9. *At. Data Nucl. Data Tables* 17:411 (1976).
10. J. E. Monahan and F. J. D. Serduke, *Phys. Rev. C*, 17:1196 (1977).